

Influence of inlet geometry on mixing in thermocline thermal energy storage

YOUSEF H. ZURIGAT,† PEDRO R. LICHE and AFSHIN J. GHAJAR‡

School of Mechanical and Aerospace Engineering, Oklahoma State University, Stillwater, OK 74078, U.S.A.

(Received 30 August 1989 and in final form 13 February 1990)

Abstract—In this study, the influence of inlet geometry on the degree of stratification attainable in thermocline thermal energy storage is investigated. The turbulent mixing caused by different inlet geometries is quantified using a mixing index introduced in a one-dimensional flow model. The mixing index is correlated with the flow parameters for three different inlet configurations. Based on the obtained correlations it is concluded that the inlet geometry starts to influence thermal stratification in a thermocline thermal storage tank for Richardson numbers below 3.6.

INTRODUCTION

Thermal storage is an effective energy management technique widely used in energy conservation and load management applications. A number of concepts have been developed for hot or cold storage in either sensible or latent forms. Many storage materials have been tested and/or used [1, 2]. Water, owing to its abundance, low cost, high specific heat and benign character, is the most widely used storage medium in low-to-medium temperature sensible thermal storage applications.

Chilled or hot water is stored in tanks which vary in design (see ref. [3]) as dictated by different factors, such as thermal performance and architectural, retrofit, and economical constraints. The single stratified tank is likely to be the most promising thermal storage device owing to its simplicity, reliability [4] and potential for high performance [5]. In a single stratified tank both hot and cold water are stored with no physical barrier in between. Buoyancy is the only mechanism separating the hot and cold water resulting in a region of steep temperature gradient called a 'thermocline', hence, thermocline thermal energy storage. This thermocline migrates from top to bottom (charge of hot water or discharge of chilled water) or from bottom to top of the tank (discharge of hot water or charge of chilled water).

The single stratified tank has been the subject of experimental and theoretical investigations [5-16]. The effect of several geometric and dynamic parameters on thermal stratification, i.e. inlet port location and geometry, mass flow rate, length to diameter ratio and inlet and outlet water temperature

difference have been studied, and the results expressed in terms of the extraction efficiency [6]. The position and sharpness of the thermocline were found to be a function of the Richardson and Peclet numbers, and a critical value of the Richardson number of 0.244 was found to be the limit below which stratification does not occur [7]. The one-dimensional nature of the flow in a thermocline tank was confirmed by radial measurements of the temperature distribution in the tank [8]. Conduction through the insulation to the ambient was found to be a larger loss mechanism than conduction across the thermocline, especially in slender tanks [9].

Numerical studies were conducted using models of varying complexity [10-16]. Comparison between one- and two-dimensional models has been reported by Cabelli [10] and Jaluria and Gupta [11]. It was found that the discrepancy between the predictions of the two models is small. The numerical study of Guo and Wu [12] has shown that a high degree of stratification will develop when Richardson number is greater than unity.

While the two- and three-dimensional models are more capable of accounting for different factors affecting thermal storage tank performance, they are not suitable for use in large energy systems simulation. The one-dimensional models, while less accurate, are computationally more efficient. Their accuracy, however, could be improved by introducing empirically-based functions accounting for departures from one-dimensional flow behavior or by using design measures that make the flow predominantly one-dimensional.

Based on purely physical arguments, one would require the flow in a thermocline thermal storage tank to be one-dimensional since any motion in the second or third directions would only enhance mixing and widen the thermocline appreciably. The achievement of one-dimensional flow in a thermocline storage tank

† Present address: ESM Department, Virginia Polytechnic Institute and State University, Blacksburg, VA 24061, U.S.A.

‡ Author to whom correspondence should be addressed.

NOMENCLATURE

A	tank cross-sectional area	x	vertical distance.
C	Courant number, $V_m \Delta t / \Delta x$	Greek symbols	
C_p	specific heat	α	molecular thermal diffusivity,
D	tank inside diameter	$\rho C_p / K$	
d	hydraulic diameter of the inlet port	$\Delta \rho$	absolute density difference between
Fo	Fourier number, $\alpha \Delta t / \Delta x^2$		initial (ambient) and inlet conditions
g	acceleration of gravity	ΔT	absolute temperature difference between
H	effective height between inlet and the last thermocouple level		initial and inlet conditions
K	thermal conductivity	ϵ_H	eddy diffusivity, $\rho C_p / K_t$
K_t	eddy conductivity	ϵ_{eff}	effective diffusivity factor,
L	height of the test tank		$(\alpha + \epsilon_H) / \alpha$
N_{sl}	number of finite difference grid points	μ	dynamic viscosity
N_{st}	total number of grid points	ρ	density.
P	tank inside perimeter	Subscripts	
Re	Reynolds number, $\rho_m V_m d / \mu_m$	a	ambient
Ri	Richardson number, $\Delta \rho g H / \rho_m V_m^2$	in	inlet
T	temperature	m	mean value evaluated at the average of the initial and inlet temperatures
T^*	dimensionless temperature, $(T - T_0) / (T_{in} - T_0)$	n	at point n
t	time	0	initial.
t^*	dimensionless time, $t V_m / H$	Superscripts	
V_{in}	mean velocity from the inlet port	'	at new time step
V_m	mean vertical velocity in the tank	in	value at the inlet.
U	overall heat transfer coefficient based on the tank inside surface area		

is possible by proper design of inlet diffusers. In this case, mixing still exists but in a limited region in the tank, namely, the inlet region where three-dimensional effects are significant. Other investigators have recognized this and included the mixing effects in different ways in their one-dimensional models, i.e. Cole and Bellinger [15], Wildin and Truman [5], and Oppel *et al.* [16]. The comparison between these and other models can be found in ref. [17].

The turbulent mixing during charge and discharge cycles is one of the major contributors to the loss of thermodynamic availability of stored energy. Other mechanisms contributing to the loss of stored energy are (1) the heat loss to the ambient surroundings, (2) thermal diffusion in the fluid body, and (3) vertical conduction in the tank wall and the associated convective motions. Consistent with the scope of this paper, the first and third mechanisms were made insignificant in the experiments by using an insulated thin-wall tank. In addition the duration of the experiments was of the order of 1 h. Thus the conduction in the fluid body and the thermal capacity of the wall were not influential factors in the development of thermocline after its formation at the inlet. This leaves the inlet geometry as the determining factor which is the case investigated in this study. The mixing at the inlet remains difficult to evaluate since it is inlet design dependent among other factors. In this study the tur-

bulent mixing in thermocline thermal storage tanks is quantified by means of an effective diffusivity factor introduced in a one-dimensional analytical model. As shown in the next section, this factor has the effect of magnifying the molecular thermal diffusivity to include turbulent mixing. Experiments with hot-cold water in a thermocline thermal storage tank were conducted to correlate the effective diffusivity factor with the flow parameters and inlet configurations. The model in which the effective diffusivity factor was introduced is discussed next.

EFFECTIVE DIFFUSIVITY MODEL

The flow in a stratified tank is modeled by the one-dimensional turbulent energy equation with heat loss to the ambient surroundings:

$$\frac{\partial T}{\partial t} + V \frac{\partial T}{\partial x} = \frac{\partial}{\partial x} \left(\alpha \epsilon_{eff} \frac{\partial T}{\partial x} \right) + \frac{UP}{A \rho C_p} (T_a - T) \quad (1)$$

where

$$\epsilon_{eff} = (\alpha + \epsilon_H) / \alpha$$

is an effective diffusivity factor.

Equation (1) can be expanded as

$$\frac{\partial T}{\partial t} + V \frac{\partial T}{\partial x} = \alpha_{\text{eff}} \frac{\partial^2 T}{\partial x^2} + \alpha \frac{\partial T}{\partial x} \frac{\partial \epsilon_{\text{eff}}}{\partial x} + \frac{UP}{A\rho C_p} (T_a - T). \quad (2)$$

Our previous experiments [16, 18] showed that the thermocline profiles away from the inlet are parallel, indicating negligible mixing after the formation of thermocline at the tank inlet region (see Figs. 5–7). This is typical of the type of experiments conducted in this study as mentioned in the previous section. Therefore, the variation of ϵ_{eff} with height was modeled by a decreasing hyperbolic function. Accordingly, the term $\partial \epsilon_{\text{eff}}/\partial x$ is appreciable only at the inlet and is negligible elsewhere. This was verified by calculating the thermocline profiles with and without the $\partial \epsilon_{\text{eff}}/\partial x$ term in equation (2). Comparison of the calculated profiles showed that this omission did not introduce appreciable error in the calculations. Therefore, the second term on the right-hand side of equation (2) was omitted for the sake of simplicity in the analysis presented here. Thus, equation (2) becomes

$$\frac{\partial T}{\partial t} + V \frac{\partial T}{\partial x} = \alpha_{\text{eff}} \frac{\partial^2 T}{\partial x^2} + \frac{UP}{A\rho C_p} (T_a - T). \quad (3)$$

Note that for laminar flow $\epsilon_{\text{eff}} = 1$ everywhere and $\epsilon_{\text{eff}} = 1$. For turbulent flow ϵ_{eff} is much greater than unity. This is equivalent to stating that the molecular thermal diffusivity, α , is magnified by turbulence by a factor of ϵ_{eff} .

A finite-difference solution technique is used to solve equation (3) subject to the appropriate initial and boundary conditions. The heat losses from the top and bottom of the tank were neglected. To eliminate the numerical diffusion inherent in the upwind differencing of the first derivative (convective term), equation (3) is split into two cases. These are the diffusion case

$$\frac{\partial T}{\partial t} = \alpha_{\text{eff}} \frac{\partial^2 T}{\partial x^2} + \frac{UP}{A\rho C_p} (T_a - T) \quad (4)$$

and the convection case

$$\frac{\partial T}{\partial t} + V \frac{\partial T}{\partial x} = 0. \quad (5)$$

Implicit finite-difference representation of equation (4) yields the system of equations

$$(-\epsilon_{\text{eff}} Fo) T'_{n-1} + (1 + \phi + 2\epsilon_{\text{eff}} Fo) T'_n + (-\epsilon_{\text{eff}} Fo) T'_{n+1} = \phi T_a + T_n \quad (6)$$

where

$$\phi = \frac{UP\Delta t}{A\rho C_p} = \frac{4U\Delta t}{D\rho C_p}.$$

Explicit finite-difference representation of equation (5) gives

$$T''_n = T_n - \frac{V\Delta t}{\Delta x} (T_n - T_{n-1}). \quad (7)$$

Here double prime denotes new values that may be calculated at a different time step than that in equation (6).

To obtain the exact solution of equation (5), the Courant number, $C = V_m \Delta t / \Delta x$, should be equal to unity, which is also the stability limit [19]. This gives

$$T''_n = T_{n-1}. \quad (8)$$

For the variable flow rate case, C could be different from unity. Therefore, the 'buffer tank' concept [16] was used. This mathematical concept is based on setting C equal to unity by the choice of Δx or Δt for the maximum expected flow rate, and applying equation (8) only at multiples of Δt for which C is equal to unity for other flow rates. For example if $C = 1/2$, equation (8) would be applied every other time step.

The problem remains in the choice of ϵ_{eff} in equation (4). Since different inlets promote turbulence in a varying degree, it is expected that ϵ_{eff} will assume different values for different inlets. Based on experiments with fresh-saline water systems [16, 18], ϵ_{eff} was found to vary spatially from a maximum at the inlet ($\epsilon_{\text{eff}}^{\text{in}}$) to a minimum of unity at the outlet in a decreasing hyperbolic function of the form (other functions were also tried, i.e. linear and exponential)

$$\epsilon_{\text{eff}} = A/N_{\text{sl}} + B \quad (9)$$

where

$$A = (\epsilon_{\text{eff}}^{\text{in}} - 1)/(1 - 1/N_{\text{sl}})$$

$$B = \epsilon_{\text{eff}}^{\text{in}} - A.$$

The total number of slabs, N_{sl} , is determined by

$$N_{\text{sl}} = H/(V_m \Delta t). \quad (10)$$

A problem thus remains in specifying the inlet value of the effective diffusivity factor, $\epsilon_{\text{eff}}^{\text{in}}$. Figure 1 shows the model's predictions of the transient temperature profiles at a certain location in the tank ($x/L = 0.657$) for different values of $\epsilon_{\text{eff}}^{\text{in}}$ for an arbitrary condition

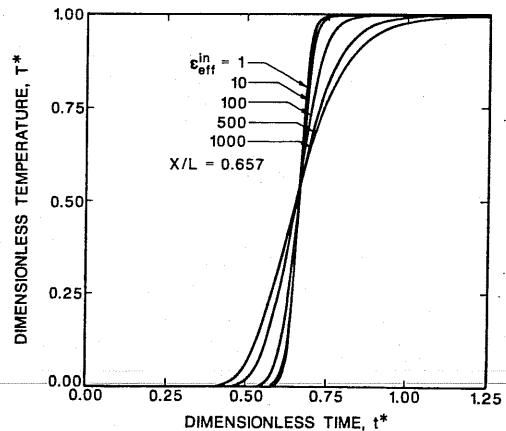


FIG. 1. Thermocline shape for different values of $\epsilon_{\text{eff}}^{\text{in}}$.

(flow rate, T_0 and T_{in}). It is seen that the thermocline gets thicker as e_{eff}^{in} increases. This indicates that:

(1) The effective diffusivity factor can represent the modifying effect of turbulence if expressed in terms of flow parameters and physical conditions.

(2) This factor may serve as a tool to quantify the turbulent mixing and thus, may be used to identify the best inlet configuration for high performance.

The objective of this study is to quantify the turbulent mixing in thermocline thermal storage tanks by specifying the inlet effective diffusivity factor, e_{eff}^{in} , for different flow conditions and types of inlets. This is done by using experimental data obtained at our laboratory from a hot-cold water system with three different inlet configurations.

EXPERIMENTS

The experimental setup is shown schematically in Fig. 2. It consists of a hot water supply tank equipped with two heaters, insulated steel test tank, metered flow system, temperature sensor arrays, and data acquisition system.

The hot water supply tank is capable of supplying hot water at any desired temperature up to 93.3°C (200°F). The test tank [40.64 cm (16 in.) diameter, 144.65 cm (56.95 in.) high and 0.254 cm (0.1 in.) thick wall wrapped with 7.62 cm (3 in.) of fiberglass insulation of 3.7 R-value] is equipped with an inlet adapter to facilitate the installation of different inlet diffusers. Three different inlet geometries were tested (see Fig. 3):

(1) Side inlet: 1.61 cm (0.634 in.) i.d. pipe located at 5.51 cm (2.17 in.) from the pipe center to the top of the tank and extending 1.93 cm (0.76 in.) into the tank.

(2) Side inlet with perforated baffle (perforated inlet): a perforated circular baffle [40 cm (15.75 in.) diameter, with 482 holes each 0.51 cm (0.201 in.) in diameter] was installed 1.27 cm (0.5 in.) below the side inlet described above.

(3) Impingement inlet: 1.8 cm (0.709 in.) i.d. pipe entering the side of the tank, turning upwards approximately 1.0 cm (0.4 in.) from the top surface of the tank with the flow impinging on the center of the top side of the tank.

Thermocline experiments (constant inlet temperature) were carried out for the charging mode of operation (hot water fed to the top of the tank and cold water withdrawn from the bottom) with flow rates ranging from 1.89 to 11.36 l min⁻¹ (0.5–3.0 gpm) and temperature differences of 22.2–66.7°C (40–120°F). Accordingly, the Reynolds and Richardson numbers were varied from 3000 to 20000 and 0.50 to 20.0, respectively. The flow rate was monitored using a calibrated rotameter with full scale accuracy of ±2% and full scale repeatability of ±1%. However, since the experiments were of constant flow rate type, the rotameter was used primarily to set the desired flow rate and a more accurate flow rate measurement technique was used. That is, a scaled catch tank was used to measure the volume of water displaced during each experimental run. The measured volume (to within ±0.5 l) was then divided by the run time to give the average flow rate. Transient temperature profiles inside the test tank were measured using 36 J-type thermocouples mounted at nine levels with four thermocouples at each level. At each level, each two opposite thermocouples were extended 5.08 and 7.62 cm (2 and 3 in.), respectively. The first level is located at 12.45 cm (4.9 in.) below the top of the tank (just below the inlet adapter flange). The rest of the levels are located at 13.7 cm (5.4 in.) intervals down the tank

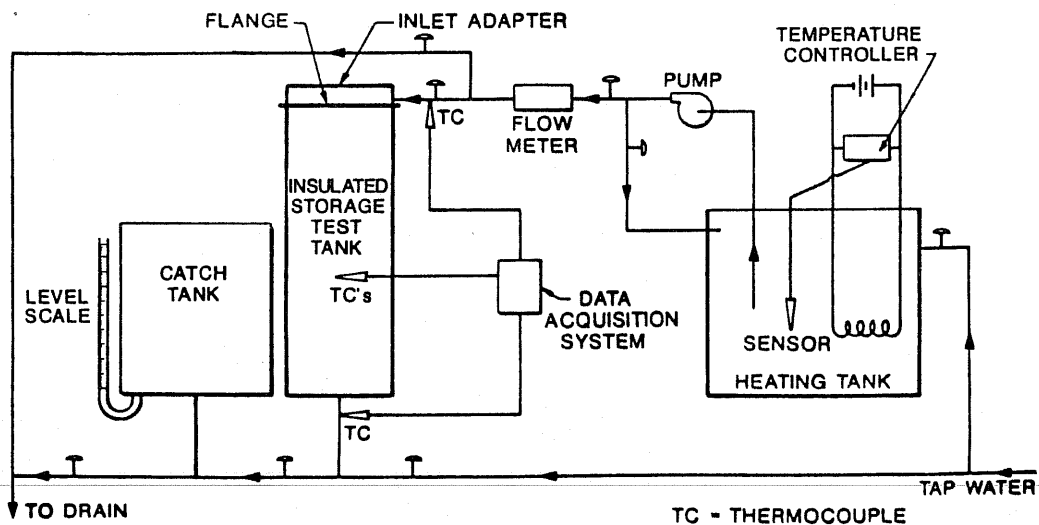


FIG. 2. Schematic of the experimental setup for hot-cold water system.

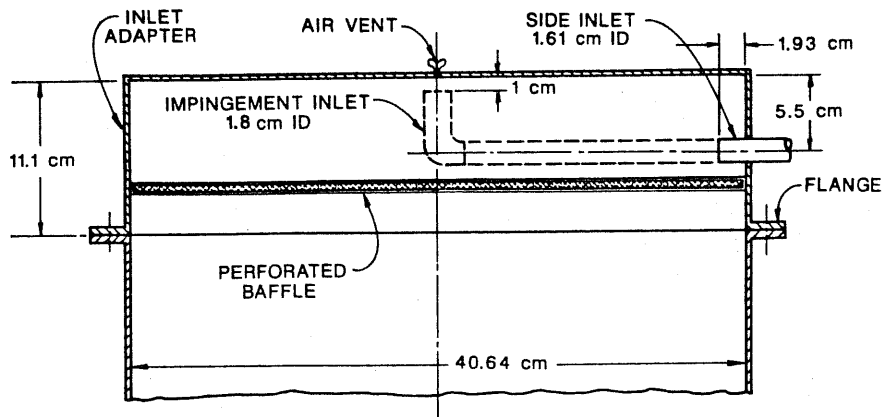


FIG. 3. Schematic of the inlet configurations tested.

(see Fig. 4). Four more thermocouples were used to measure the hot water supply tank, test tank inlet and outlet and the ambient temperatures.

The data acquisition system used consists of a 40 channel Monitor Labs model 9302 data logger interfaced with a TI computer. Temperature readings were taken at 20–40 s intervals. Figures 5–7 show typical transient temperature profiles by levels after averaging the four readings at each level. Calibration of thermocouples showed that the measurements were accurate within $\pm 0.56^\circ\text{C}$ ($\pm 1^\circ\text{F}$). The data reduction software written in C-language and the data acquisition system are described in Rao *et al.* [20].

RESULTS AND DISCUSSION

The influence of the inlet geometry on stratification in a thermocline thermal storage tank was recognized in earlier studies [5, 6, 18]. The experiments conducted in this study confirm such influence as can be seen in Figs. 5–7 for the three inlet configurations tested at nearly identical inlet to initial temperature difference (note that the flow rate for the side inlet is less than those for the other inlets). In this study, however, an attempt is made to quantify the turbulent mixing introduced by different inlet geometries. Based on this quantification three objectives can be realized: (1) identification of the best inlet configuration for enhancement of stratification in a storage tank, (2) development of mixing correlations to be used in a simple one-dimensional model, and (3) establishment of the conditions under which the influence of the inlet geometry diminishes.

The effective diffusivity factor introduced in an earlier section is considered as the starting point in achieving the above objectives. This factor was specified based on the experimental data. For any set of data an initial value of $\epsilon_{\text{eff}}^{\text{in}}$ is assumed and the thermocline is calculated based on the model discussed earlier. Comparison of the predicted thermocline for different values of $\epsilon_{\text{eff}}^{\text{in}}$ with the experimentally obtained thermocline, establishes the best choice for $\epsilon_{\text{eff}}^{\text{in}}$. It should be pointed out that this best choice of $\epsilon_{\text{eff}}^{\text{in}}$ usually produced a varying degree of agreement with the experimental data at different levels in the tank. At low flow rates [i.e. less than $2\text{--}3\text{ l min}^{-1}$ ($0.53\text{--}0.79\text{ gpm}$)] good agreement was achieved throughout the tank. However, at higher flow rates it was not possible to obtain good predictions of the temperature profiles at all the levels with a single value of $\epsilon_{\text{eff}}^{\text{in}}$. High values of $\epsilon_{\text{eff}}^{\text{in}}$ were necessary for good predictions at the first few levels but these resulted in poor agreement in the rest of the tank. Since one of the major assumptions used in the model is that of the flow being one-dimensional, good predictions in the regions where two- and three-dimensional effects may be present (the inlet region) are difficult to achieve. Therefore, the $\epsilon_{\text{eff}}^{\text{in}}$ was

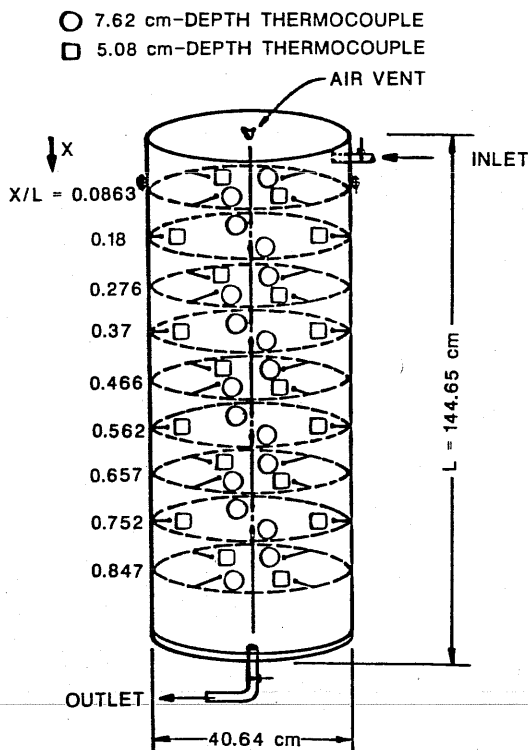


FIG. 4. Test tank thermocouples layout.

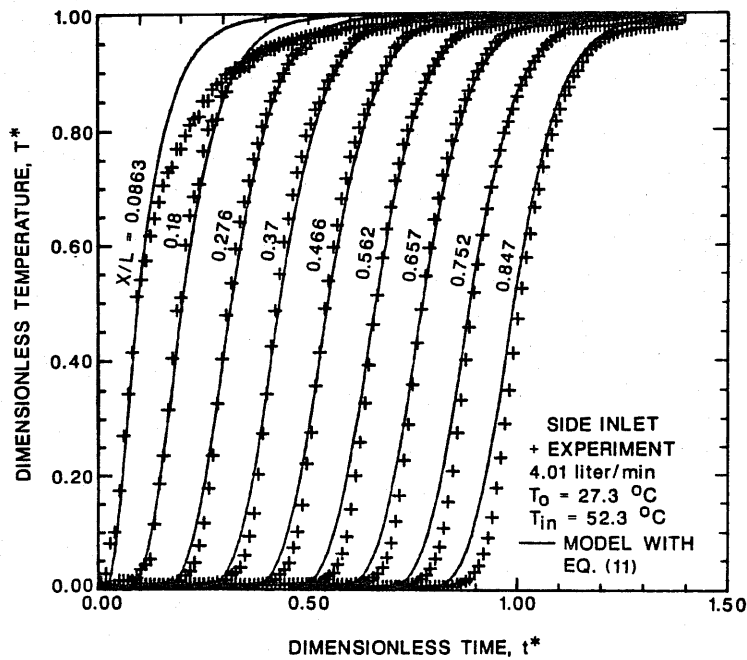


Fig. 5. Measured and predicted transient temperature profiles at different locations in the test tank (side inlet).

optimized to produce good predictions at the last five to six levels in the tank. This is justified since in many cases (i.e. energy systems simulations) the outlet temperature is of prime interest. Using the outlined procedure the values of $\epsilon_{\text{eff}}^{\text{in}}$ that produce the best prediction of the experimental data were obtained for all

the experiments conducted in this study (total of 40 experiments).

The inlet effective diffusivity factor was shown [18] to increase as the flow rate increases and decrease as the temperature difference, ΔT , increases. This points to two dimensionless numbers as having the con-

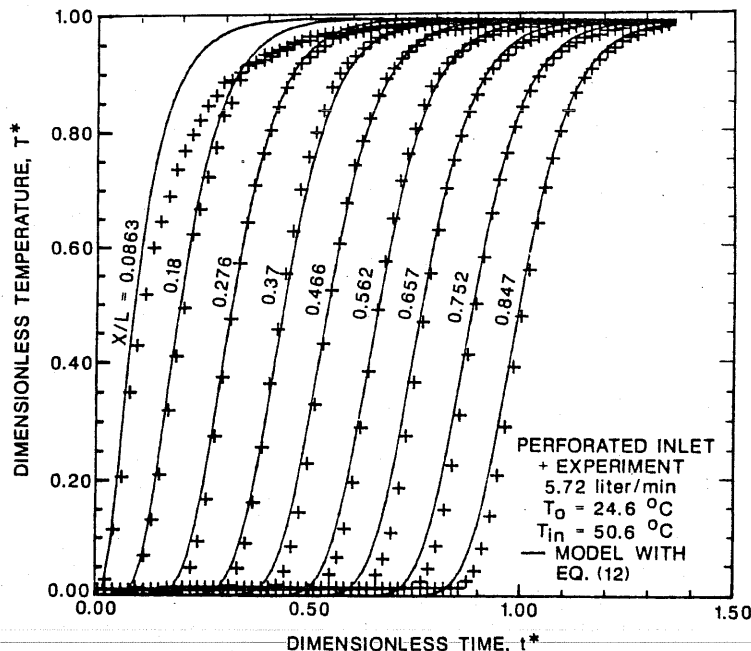


Fig. 6. Measured and predicted transient temperature profiles at different locations in the test tank (perforated inlet).

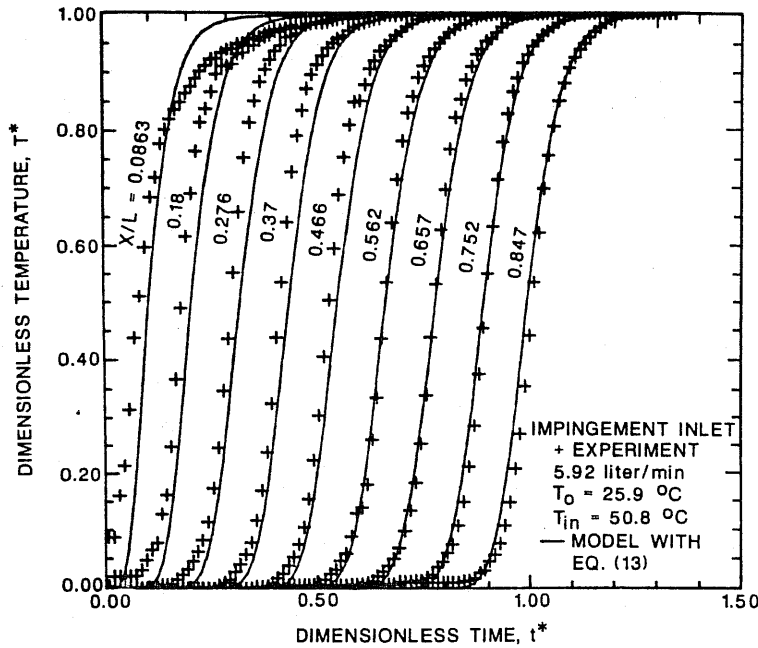


FIG. 7. Measured and predicted transient temperature profiles at different locations in the test tank (impingement inlet).

trolling effect on stratification in thermocline thermal storage tanks, namely; Reynolds and Richardson numbers. While the former represents the degree of turbulence introduced at the inlet, the latter represents the degree of turbulence suppression. Stable stratification has a modifying effect on turbulence since it damps out the eddy transport of momentum and heat, especially the latter.

Based on the foregoing discussion the inlet effective diffusivity factor was correlated with the ratio of Reynolds to Richardson numbers. It should be noted that while the effect of viscosity on the mixing process is negligible at the Reynolds number range tested, the choice of this ratio in correlations is more convenient for visualizing the influence of each inlet geometry and provides more accurate curve-fits. In addition, the choice of tank height as the length scale in the definition of the Richardson number (see Nomenclature) facilitates comparison of the results of this study with the results available in the literature, such as refs. [9, 22]. Figure 8 shows the correlations obtained for the corresponding inlet configurations:

for side inlet

$$\epsilon_{\text{eff}}^{\text{in}} = 0.344(Re/Ri)^{0.894}; \quad (11)$$

for perforated inlet

$$\epsilon_{\text{eff}}^{\text{in}} = 3.54(Re/Ri)^{0.586}; \quad (12)$$

for impingement inlet

$$\epsilon_{\text{eff}}^{\text{in}} = 4.75(Re/Ri)^{0.522}. \quad (13)$$

Equations (11)–(13) represent the curve-fits of $\epsilon_{\text{eff}}^{\text{in}}$ values obtained based on the procedure described

earlier in this section. Equation (11) correlates the 12 data points for the side inlet with an average absolute error of 22% and a maximum absolute error of 40%. The correlation predicts 33% of the data with less than 15% deviation and 67% with less than 25%. The 16 data points for the perforated inlet were correlated by equation (12) with an average absolute error of 15% and a maximum absolute error of 30%. For this case, 56% of the data had less than 15% deviation and 94% less than 25%. Finally, for the impingement inlet, equation (13) correlates the 12 data points with an average absolute error of 15% and a maximum absolute error of 36%. The correlation predicts 58% of the data with less than 15% deviation and 92% with less than 25%. The resulting error in $\epsilon_{\text{eff}}^{\text{in}}$ calculated from the obtained correlations and its sub-

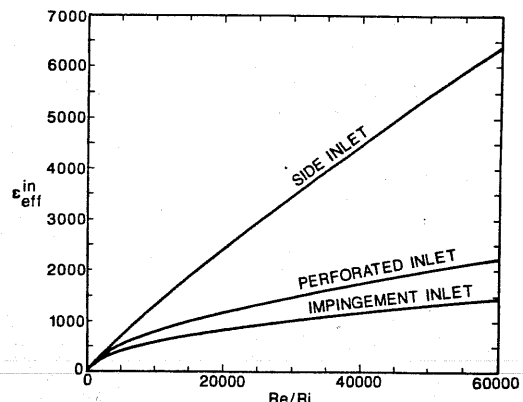


FIG. 8. Recommended correlations for $\epsilon_{\text{eff}}^{\text{in}}$ as a function of the ratio Re/Ri .

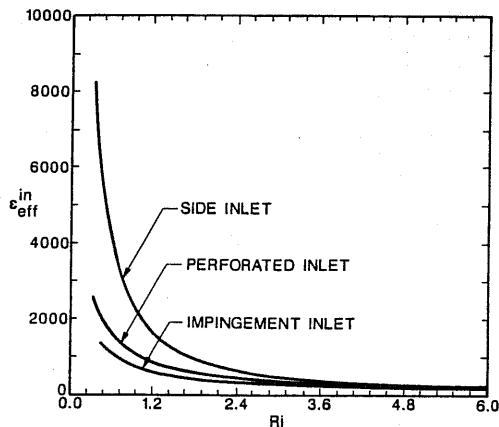


Fig. 9. Inlet effective diffusivity factor variation as a function of Richardson number.

sequent effect on the temperature profile predictions should be viewed in light of Fig. 1. It can be seen that the error in the temperature profile predictions resulting from 15 to 30% error in $\epsilon_{\text{eff}}^{\text{in}}$ is rather small and falls within the experimental accuracy. The best test, however, is to compare the predicted temperature profiles with the aid of these correlations with the experimental data. These comparisons are presented in Figs. 5–7 and in the latter part of this section (see Figs. 10–12).

By examining Fig. 8, two observations can be made: (1) the inlet that introduces the least mixing is the impingement inlet since it has the least $\epsilon_{\text{eff}}^{\text{in}}$ at all (Re/Ri) ratios considered, and (2) the use of the perforated baffle significantly reduces the turbulent mixing compared with the case of a side inlet without a baffle. The effect of the baffle is seen to be more pronounced at higher values of Re/Ri . From Fig. 8 it is also observed that at low values of Re/Ri there is little difference in the performance of the three inlet

configurations tested. Thus, the conditions under which the influence of the inlet geometry diminishes can be readily established. In previous studies [18, 21], this was expressed in terms of Richardson number alone. Based on experiments with a fresh-saline water system [18] a value of Richardson number of 5.0 was found to be the limit above which the inlet geometry has a negligible effect on thermal stratification in a thermocline thermal storage tank. A value of 9.8 was deduced by Han and Wu [21] from their numerical study. The correlations given by equations (11)–(13) and shown in Fig. 8 are replotted in Fig. 9 in terms of Richardson number alone by varying the flow rate for a fixed temperature difference, ΔT . This figure shows that at $Ri \geq 3.6$ no significant difference in the performance of the inlets tested is observed as evidenced by the minor difference and change in $\epsilon_{\text{eff}}^{\text{in}}$ values as Ri exceeds 3.6.

In view of these different results, it should be noted that there are uncertainties regarding the results of refs. [18, 21]. The result of the former was based on fresh-saline water system measurements which are rather qualitative since the temperature profiles generated from density profiles measurements are very sensitive to small changes in density. On the other hand, the results of ref. [21] were based on qualitative comparisons of the flow patterns generated by a two-dimensional laminar flow model. Therefore, it is believed that the result obtained in the present study represents the limit beyond which the inlet geometry has a negligible effect on thermal stratification in a thermocline thermal storage tank.

Based on the above result it can be concluded that one-dimensional modeling may break down for $Ri < 3.6$ and hence, mixing correlations for particular inlet configurations are necessary if the operating conditions require $Ri < 3.6$. It is, therefore, of interest to compare the predictions of the model presented in an earlier section [with $\epsilon_{\text{eff}}^{\text{in}}$ in equation (9) calculated from

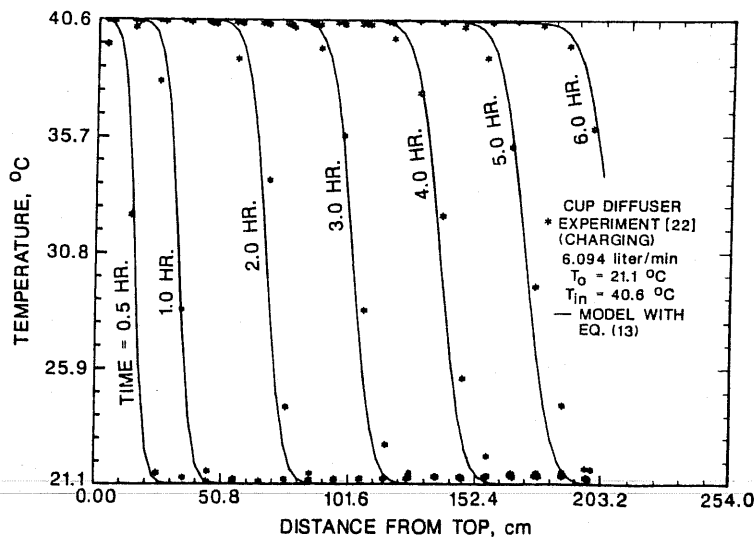


Fig. 10. Predicted temperature profiles compared with experimental data from Kuhn *et al.* [22] (charging).

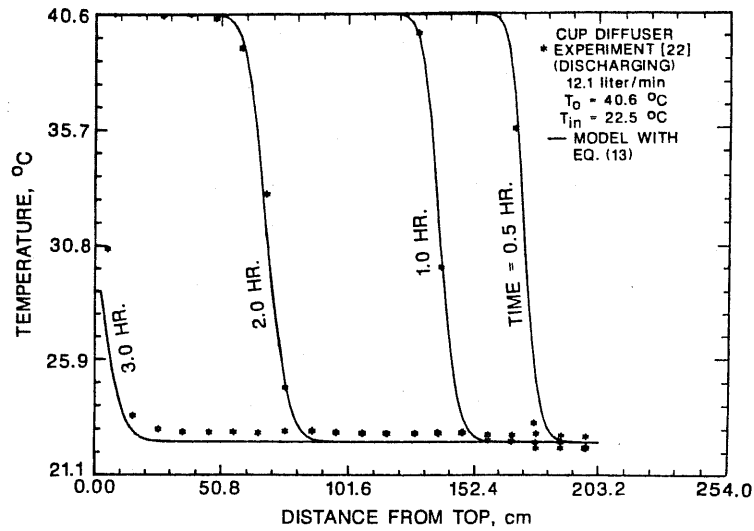


FIG. 11. Predicted temperature profiles compared with experimental data from Kuhn *et al.* [22] (discharging).

the corresponding correlations, i.e. equations (11)–(13)] with our experimental data and those from the literature [9, 22]. Figures 5–7 and 10–12 show the predictions of the model with the experimental data of the sources indicated. It can be seen that a good agreement between the predicted thermocline and the experimental one is achieved. Thus, a complete model of the thermocline thermal storage tank incorporating mixing correlations for three types of inlet geometry is now available. It should be noted that in the presence of two- and three-dimensional effects (low values of Ri or high values of Re) no one-dimensional theory can be applied with equal success to different inlet

geometries without the use of mixing correlations for different inlets. Therefore, the correlations presented in this study are essential for better predictions in one-dimensional thermocline computations. This should provide a reliable guidance to the designers of thermocline thermal storage tanks for the choice of the type of inlet to use depending on the operating conditions desired.

SUMMARY AND CONCLUSIONS

The degree of stratification attainable in thermocline thermal energy storage is generally influenced.

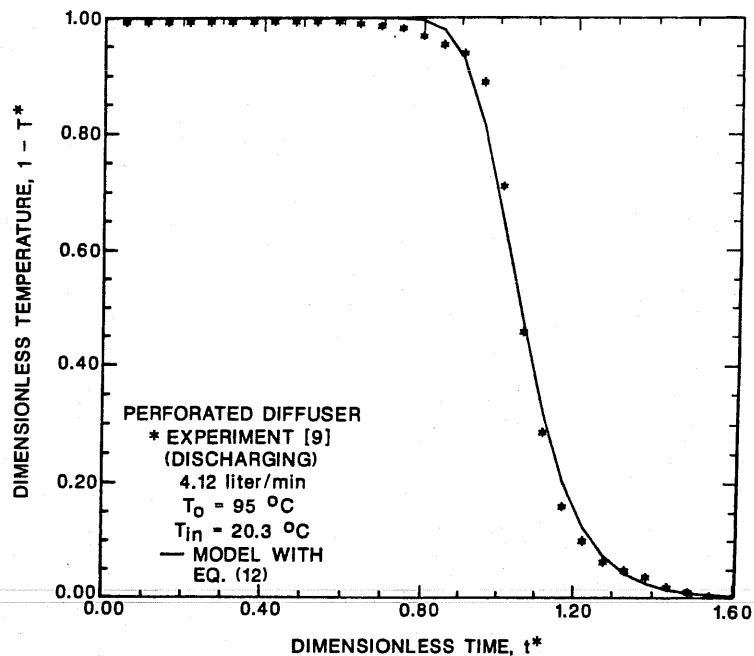


FIG. 12. Predicted temperature profile compared with experimental data from Abdoly [9] (discharging).

among other factors, by the inlet geometry. In this study turbulent mixing caused by three different inlet configurations was investigated. Quantification of turbulent mixing was made based on an effective diffusivity factor introduced by one-dimensional flow modeling. This factor was shown to serve as a practical measure for characterization of inlet-geometry-induced mixing. Mixing correlations for the three inlet configurations were obtained based on experiments with a hot-cold water system. The one-dimensional model incorporating these correlations was shown to satisfactorily reproduce the experimental data of ours and of other investigators. Based on the obtained correlations it was concluded that the influence of the inlet geometry on stratification is negligible for Richardson number above 3.6. Thus the one-dimensional flow modeling without accounting for the mixing at the inlet may break down at Richardson numbers below 3.6 and mixing correlations for individual inlet geometries would be necessary if operating Richardson numbers below 3.6 were to be employed.

Acknowledgement—Support for this research provided by the Oklahoma State University Center for Energy Research under Grant No. 1150726 is gratefully acknowledged.

REFERENCES

1. C. S. Herrick, H. Jaster, R. S. Miller and R. Williams, Cool storage assessment study, EPRI Report, EPRI EM-468, 2-17-2-24 (1977).
2. E. C. Guyer and D. L. Brownwell, Review of heat storage materials, EPRI Report, EPRI EM-3353 (1983).
3. R. T. Tamblyn, Thermal storage resisting temperature blending, *ASHRAE J.* **22**, 65-70 (1980).
4. D. S. Seth and R. G. Leduc, Daily thermal energy storage: Canadian experience, EPRI EM-3159-SR, Special Report on Opportunities in Thermal Storage R&D, P7-1-P7-9 (1983).
5. M. W. Wildin and C. R. Truman, Evaluation of stratified chilled-water storage technique, EPRI Report, EPRI EM-4352 (1985).
6. Z. Lavan and J. Thompson, Experimental study of thermally stratified hot water storage tanks, *Sol. Energy* **19**, 519-524 (1977).
7. B. J. Sliwinski, A. R. Mech and T. S. Shih, Stratification in thermal storage during charging, *Proc. Sixth Int. Heat Transfer Conf.*, Vol. 4, pp. 149-154. American Society of Mechanical Engineers (1978).
8. R. J. Gross, An experimental study of single medium thermocline thermal energy storage, ASME Paper 82-HT-53 (1982).
9. M. A. Abdoly, Thermal stratification in storage tanks, Ph.D. thesis, University of Texas at Dallas (1981).
10. A. Cabelli, Storage tanks—a numerical experiment, *Sol. Energy* **19**, 45-54 (1977).
11. Y. Jaluria and S. K. Gupta, Decay of thermal stratification in a water body for solar energy storage, *Sol. Energy* **28**, 137-143 (1982).
12. K. L. Guo and S. T. Wu, Numerical study of flow and temperature stratification in a liquid storage tank, *ASME J. Sol. Energy Engng* **107**, 15-20 (1985).
13. W. F. Phillips and R. A. Pate, Mass and energy transfer in a hot liquid energy storage system, *Proc. AISES*, Oakland, Florida, pp. 17-6 and 17-10 (1977).
14. W. T. Sha and E. I. H. Lin, Three dimensional mathematical model of flow stratification in thermocline storage tanks. In *Application of Solar Energy* (Edited by S. T. Wu *et al.*), p. 185 (1978).
15. R. L. Cole and F. O. Bellinger, Thermally stratified tanks, *ASHRAE Trans.* **88**, 1005-1017 (1982).
16. F. J. Oppel, A. J. Ghajar and P. M. Moretti, A numerical and experimental study of stratified thermal storage, *ASHRAE Trans.* **92**, 293-309 (1986).
17. Y. H. Zurigat, K. J. Maloney and A. J. Ghajar, A comparison study of one-dimensional models for stratified thermal storage tanks, *ASME J. Sol. Energy Engng* **111**, 204-210 (1989).
18. Y. H. Zurigat, A. J. Ghajar and P. M. Moretti, Stratified thermal storage tank inlet mixing characterization, *Appl. Energy* **30**, 99-111 (1988).
19. P. J. Roache, On artificial viscosity, *J. Comp. Phys.* **10**, 169-184 (1972).
20. K. S. S. Rao, Y. H. Zurigat and A. J. Ghajar, A micro-computer-based data acquisition system and software for thermal studies, *Heat Transfer Engng* **9**, 58-66 (1988).
21. S. M. Han and S. T. Wu, Enhancement of thermal stratification in a liquid storage tank by a horizontal baffle. In *Fundamentals of Forced and Mixed Convection*, a collection of papers presented at the 23rd Natn. Heat Transfer Conf., Denver, Colorado (Edited by F. A. Kulacki and R. D. Boyd), pp. 197-205 (1985).
22. J. K. Kuhn, G. F. von Fuchs and A. P. Zob, Developing and upgrading of solar-system thermal-energy-storage simulation models, Final Report, prepared by Boeing Computer Services Company for the Department of Energy, Contract DE-AC02-77CS 34482 (1980).

INFLUENCE DE LA GEOMETRIE D'ENTREE SUR LE MELANGE DANS LE STOCKAGE DE CHALEUR THERMOCLINE

Résumé—On étudie l'influence de la géométrie d'entrée sur le degré de stratification dans un stockage de chaleur thermocline. Le mélange turbulent causé par différentes géométries d'entrée est quantifié en utilisant un indice de mélange introduit dans un modèle d'écoulement monodimensionnel. L'indice de mélange est relié aux paramètres d'écoulement pour trois configurations d'entrée. A partir des corrélations obtenues, on conclut que la géométrie d'entrée commence à influencer la stratification thermique dans un réservoir à thermocline pour des nombres de Richardson inférieurs à 3,6.

EINFLUSS DER EINLAUFGEOMETRIE AUF DIE VERMISCHUNG IN EINEM GESCHICHTETEN WÄRMESPEICHER

Zusammenfassung—Der Einfluß der Einlaufgeometrie auf den Grad der Schichtung, der sich in einem Schichtspeicher erreichen läßt, wird in der vorliegenden Arbeit untersucht. Die turbulente Vermischung durch verschiedene Einlaufgeometrie wird mit Hilfe eines Mischungsparameters qualitativ beschrieben, der in ein eindimensionales Strömungsmodell eingebaut wird. Der Mischungsparameter wird mit den Strömungsparametern der drei verschiedenen Einlaufanordnungen korreliert. Aufgrund der Korrelationen ergibt sich, daß die Einlaufgeometrie die Schichtung in einem Schichtspeicher für eine Richardson-Zahl kleiner 3,6 zu beeinflussen beginnt.

ВЛИЯНИЕ ГЕОМЕТРИИ ВХОДА НА СМЕШЕНИЕ ПРИ ТЕРМОКЛИННОМ АККУМУЛИРОВАНИИ ТЕПЛОВОЙ ЭНЕРГИИ

Аннотация—Исследуется влияние геометрии входа на степень стратификации, достигаемую при термоклинном аккумулировании тепловой энергии. Посредством введения коэффициента смешения в одномерную модель течения количественно определяется турбулентное смешение, вызванное различными геометриями входа. Устанавливается зависимость между коэффициентом смешения и параметрами течения при трех различных конфигурациях входа. На основе полученных обобщенных зависимостей делается вывод о том, что геометрия входа начинает оказывать влияние на тепловую стратификацию в термоклинном аккумуляторе тепловой энергии при значениях числа Ричардсона ниже 3,6.